Journal of Applied Polymer Science

Configurational Effects on the Crystalline Morphology and Amorphous Phase Behavior in Poly(3-hydroxybutyrate) Blends with Tactic Poly(methyl methacrylate)

Hikmatun Ni'mah, Eamor M. Woo
Department of Chemical Engineering, National Cheng Kung University, Tainan, 701, Taiwan
Correspondence to: E. M. Woo (E-mail: emwoo@mail.ncku.edu.tw)

ABSTRACT: Poly(3-hydroxybutyrate) (PHB) blends with two tactic poly(methyl methacrylate)s [PMMAs; isotactic poly(methyl methacrylate) (iPMMA) and syndiotactic poly(methyl methacrylate) (sPMMA)], being chiral/tactic polymer pairs, were investigated with regard to their crystalline spherulite patterns, optical birefringence, and amorphous phase behavior with polarized optical microscopy and differential scanning calorimetry. The PHB/sPMMA and PHB/iPMMA blends exhibited upper critical solution temperatures of about 225 and 240°C, respectively, on the basis of the results of thermal analysis and phase morphology. The interactions of two constituents in the blends (PHB/iPMMA or PHB/sPMMA) were measured to be insignificantly different for the PHB/sPMMA and PHB/iPMMA blends. However, syndiotacticity in PMMA exerted a prominent effect on the alteration of the PHB spherulite morphology, whereas, by contrast, isotacticity in PMMA had almost no effect at all. At high sPMMA contents (e.g., 30 wt %) in the PHB/sPMMA blend, the spherulites were all negatively birefringent and ringless when they were crystallized at any crystallization temperature between 50 and 90°C. That is, not only was the original ring-banded pattern in the neat PHB spherulites completely disrupted, but the optical sign was also reverted completely from positively to negatively birefringent in the sPMMA/PHB blend; this was not observed in the iPMMA/PHB one. © 2013 Wiley Periodicals, Inc. J. Appl. Polym. Sci. 129: 3113–3125, 2013

KEYWORDS: amorphous; biodegradable; blends; morphology; phase behavior

Received 23 October 2012; accepted 10 January 2013; published online 18 February 2013
DOI: 10.1002/app.39016

INTRODUCTION

Nowadays, biodegradable polymers have become an attractive topic because of their environmentally friendly applications. Poly(3-hydroxybutyrate) (PHB), which is a biodegradable polymers, has been investigated since several years ago. PHB is natural aliphatic polyester produced by bacterial fermentation, and this polymer has attracted interest for some applications because of its biodegradability and biocompatibility. However, PHB shows brittleness, and this leads to narrow utilization. Blending with other polymers is one of approaches used to overcome the limitations of biodegradable polymers. There have been many studies on PHB and its blends; these include studies of their miscibility, thermal properties, crystal morphology, crystallization behavior, and applications. PHB has been reported to be miscible with poly(ethylene oxide),[1–4] low-molecular-weight poly(L-lactic acid) (PLLA),[5,6] partially miscible with poly(trimethylene adipate) and poly(butylene adipate),[7] immiscible with poly(propylene oxide) and poly(-methylene oxide) with no upper critical solution temperature (UCST), and immiscible with some aliphatic polyesters with UCSTs, such as poly(ethylene succinate) and poly(ethylene adipate).[7]

The miscibility of polymer blends can be influenced by the type of interactions between the two polymers, the molecular weight, the stereoregularity of polymers, and so forth. The chain configuration of the polymers in blends and its effect on the miscibility between two polymers have become interesting. One of polymers that has stereoregularity in its polymer chain configuration is poly(methyl methacrylate) (PMMA). Stereoregular PMMAs, including isotactic poly(methyl methacrylate) (iPMMA), atactic poly(methyl methacrylate) (aPMMA), and syndiotactic poly(methyl methacrylate) (sPMMA), are attractive polymers because of the effects of tacticity; these reflect on their physical properties, such as their glass-transition temperature (T_g),[8] specific heat and entropy,[9] and viscoelastic properties.[10] A number of studies on the miscibility of blends composed of tactic PMMA and other polymer have been reported. Blends of poly(vinylidene fluoride) with iPMMA, aPMMA, and sPMMA have been reported to be miscible with evidence of a single glass transition and a decrease in the crystallization temperature (T_c) and melting

temperature (T_m).[11] Schurer and De Boer[12] reported that a blend of poly(vinyl chloride) with iPMMA was immiscible and partially miscible with sPMMA. In contrast, Vorenkamp et al.[13] showed that poly(vinyl chloride) blends with iPMMA, aPMMA, and sPMMA, were all miscible with a lower critical solution temperature. Hsu[14,15] found that the miscibility of tactic PMMA with poly(*p*-vinyl phenol) was based on the solvent used in polymer blending. Recently, Li and Woo[16,17] reported that PLLA blended with aPMMA and sPMMA showed immiscibility with a UCST, but PLLA blended with iPMMA showed immiscibility with no UCST. Those studies pointed out that the different tacticities of polymers might have an effect on the miscibility of the blends.

Although Cimmino and coworkers[18–20] reported earlier that a blend of PHB with aPMMA was immiscible with a UCST, the effects of the tacticity of PMMA and the chirality in PHB have yet to be understood. To our knowledge, the effects of the crystalline morphology and phase miscibility of PHB with other tactic PMMAs, including sPMMA and iPMMA, have not yet been reported. In this study, blends of PHB with two different tactic PMMAs (sPMMA and iPMMA) were investigated to probe the effects of the tacticity on the PHB crystalline morphology and the blend's amorphous phase behavior. As PHB is an aliphatic polyester with chirality, it is likely that the C=O/C=O interactions in the chiral/tactic blends may be more favorably stronger between a chiral polymer and a tactic polymer than in blends of two polymers with no tacticity or chirality. A comparison was drawn to another widely studied biodegradable and chiral polymer, PLLA, for which it has been shown that the oppositely configured sPMMA tends to have more intimate interactions with chiral PLLA than does iPMMA with PLLA. That is, the effect of the PMMA tacticity is quite pronounced in the interactions and miscibility between PMMA and PLLA. In this study, the configurational effects on the blend's amorphous phase behavior were less pronounced than those on the blend's crystalline morphology.

EXPERIMENTAL

Materials and Preparation

PHB [weight-average molecular weight (M_w) = 500,000 g/mol] was purchased from Polysciences, Warrington, Pennsylvania, USA, and had a T_g onset of about −4.7°C and a T_m of about 173°C. sPMMA (M_w = 50,000 g/mol) was supplied by Scientific Polymer Products, Inc., Ontario, New York, USA, and had a T_g onset of about 121.6°C. iPMMA (M_w = 300,000 g/mol) was also purchased from Scientific Polymer Products, Inc., Ontario, New York, USA, and had a T_g onset of about 47.7°C. All of the polymer materials were used as received.

Samples of the PHB/tactic PMMA blends were prepared by solution casting with chloroform as a solvent with a concentration of 2 wt %. A drop of solution of the polymer was deposited and uniformly spread onto a microglass slide at 45°C, and the solvent was allowed to fully evaporate in the atmosphere. The dried film on the microglass slide was crystallized without a top cover glass.

Characterization

A polarized optical microscope (Nikon Optiphot-2, Tokyo, Japan) equipped with a digital camera charge-coupled device and a microscopic hot stage (Linkam THMS-600, Surrey, UK) with a TP-92 temperature programmer) was used to characterize the optical homogeneity and crystalline morphology of the blends. To monitor the phase transition, the blend samples prepared by solution casting on glass slides were heated slowly (2°C/min) from ambient temperature to the temperature below the degradation temperature of PHB and then cooled slowly (−2°C/min) to ambient temperature. The phase transformations were then recorded at the respective temperatures. To investigate the spherulitic morphology of the blend, the blend samples were held at a temperature above the clarity point for 1 min and then quickly transferred to a hot stage equilibrated at the desired T_c at which the spherulitic morphology of the blends were observed.

The T_g measurement and melt isothermal crystallization of the PHB/tactic PMMA blends were carried out on a differential scanning calorimetry (DSC) instrument (Diamond, PerkinElmer Corp., Massachusetts, USA) under a dry/inert nitrogen flow of 20 cm^3/min. For the T_g measurements, the blend samples were scanned to temperatures above UCST at heating rate of 20°C/min and held for 2 min. The blend samples were then quickly cooled in DSC at a cooling rate of 320°C/min to subambient temperatures much below the T_g for several minutes to freeze the polymer chains. The blend samples were then scanned with DSC to the temperature above the PHB T_m at a heating rate of 20°C/min to reveal their T_g. For measurement of the T_m's of the crystallized blends, the blend samples were first rapidly heated to temperatures above the UCST clarity point and held for several minutes to eliminate any previous thermal history. The blend samples were then quickly cooled to the desired T_c at a cooling rate of 320°C/min and held there isothermally until the end of crystallization. The crystallized blend samples were then scanned in DSC to a temperature above the PHB T_m at a heating rate of 10°C/min to reveal their melting endothermic peaks.

RESULTS AND DISCUSSION

Phase Behavior and Thermal Characterization

The phase behavior of the PHB blends with tactic PMMA was first examined. Figure 1 shows the optical microscopy (OM) micrographs of the phase transition from phase separation to homogeneity for 30/70 PHB/sPMMA during the heating and cooling cycles. Other compositions of the blend were also similarly examined. The results for all of the compositions were similar. For brevity, only a blend composition of 30/70 PHB/sPMMA is shown here. The as-cast sample at ambient temperature of this blend showed a wormlike structure, which indicated heterogeneity in the blend. After it was heated to 190°C, a temperature slightly higher than the PHB T_m (∼ 173°C), the OM result of the blend still exhibited wormlike domains, which are characteristic of distinct phase separation. However, when it was continuously heated to 230°C, the blend system transformed from the heterogeneous phase (two phases) to the homogeneous phase (one-phase domain) with a certain clarity point for every composition of the blend. The temperature of the clarity point was defined as the temperature at which the heterogeneous phase turned to the homogeneous phase upon heating. This clarity point was dependent on the composition of the blend system. The phase transition upon heating, as shown in Figure 1, was likely a thermodynamic UCST phenomenon. The UCST

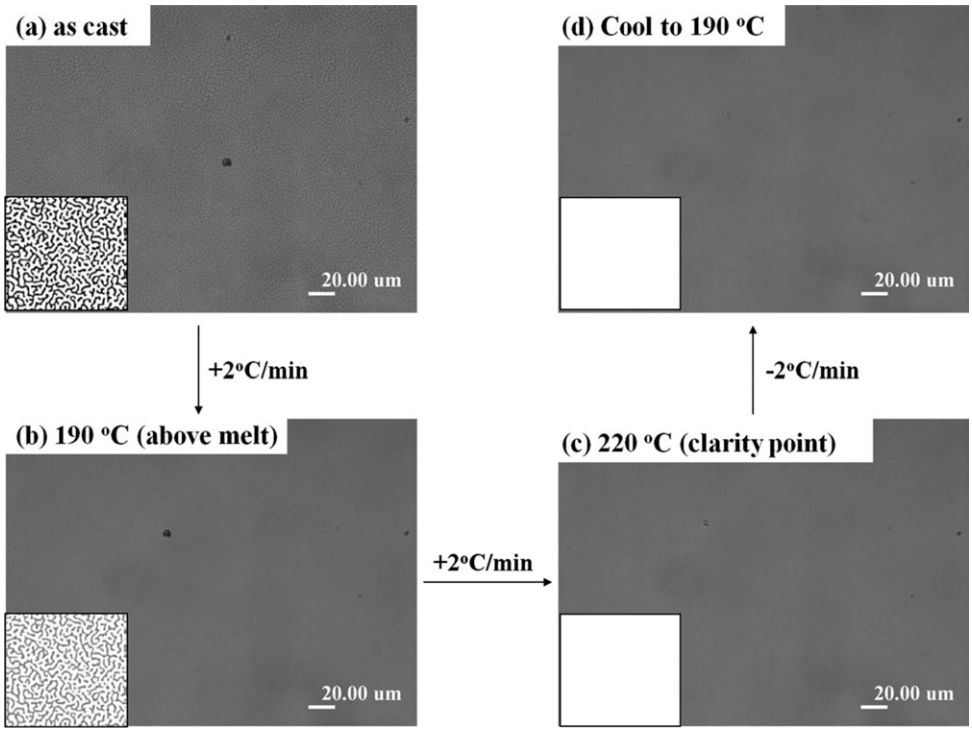

Figure 1. OM micrographs showing the phase transition upon heating and cooling cycles for the 30/70 PHB/sPMMA blend.

means that the blends revealed phase separation at lower temperatures but became one phase (miscible) at higher temperatures. When the samples were cooled back to temperatures below the UCST and above the T_m of PHB, that is, 190°C, the blends remained in the miscible state; this might have been caused by the limited chain mobility of the heat-homogenized blend above the UCST. The viscosity and entanglement might have prevented the polymer chains from rapidly reverting back to the phase separation upon cooling. The verification of the UCST reversibility is discussed in the following section.

Figure 2 shows the DSC thermographs for 30/70 PHB/sPMMA blend and UCST phase behavior in the blend system. The DSC trace for the as-cast sample displayed two T_g's, which indicated that the as-cast sample was in the phase-separated state. After it was heated to 190°C, which was above the PHB T_m, the DSC trace still showed two distinct T_g's corresponding to the T_g of each homopolymer (PHB or tactic PMMA). At that temperature, the PHB crystals were melted, and then, liquid–liquid phase separation occurred. Further heating to a temperature of 230°C (above the clarity point), the morphology of the blend was transparent; this was proven by one T_g displayed in the DSC traces.

For the PHB/iPMMA blend system, OM characterization was performed as a preliminary observation of the phase behavior. Figure 3 shows the OM micrographs of phase transition for PHB/iPMMA at a composition of 30/70 during the heating and cooling cycles. All of the blend compositions showed similar results, so for brevity, only the 30/70 PHB/iPMMA blend is shown here. The as-cast blend [Figure 3(a)] and the melting state of the blend [Figure 3(b)] showed similar results as the PHB/sPMMA blends; this showed that the blends were immiscible at ambient temperature and at above the T_m of PHB. At the UCST [Figure 3(c)], the phase domains disappeared, and the morphology of the blends became transparent; this indicated a homogeneous state. This homogeneous state remained the same when the blends were cooled to a temperature below the UCST and above T_m of PHB [Figure 3(d)]. Similar to the PHB/

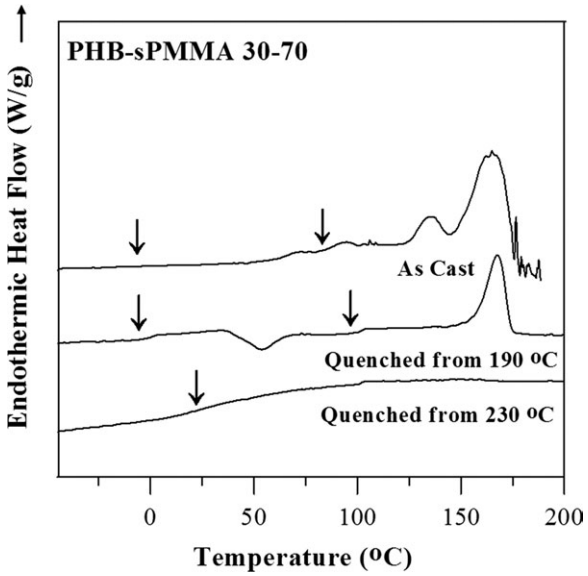

Figure 2. DSC thermographs of the 30/70 PHB/sPMMA for the as-cast blends, second scans from below the clarity point, and second scans from above the clarity point.

Applied Polymer SCIENCE

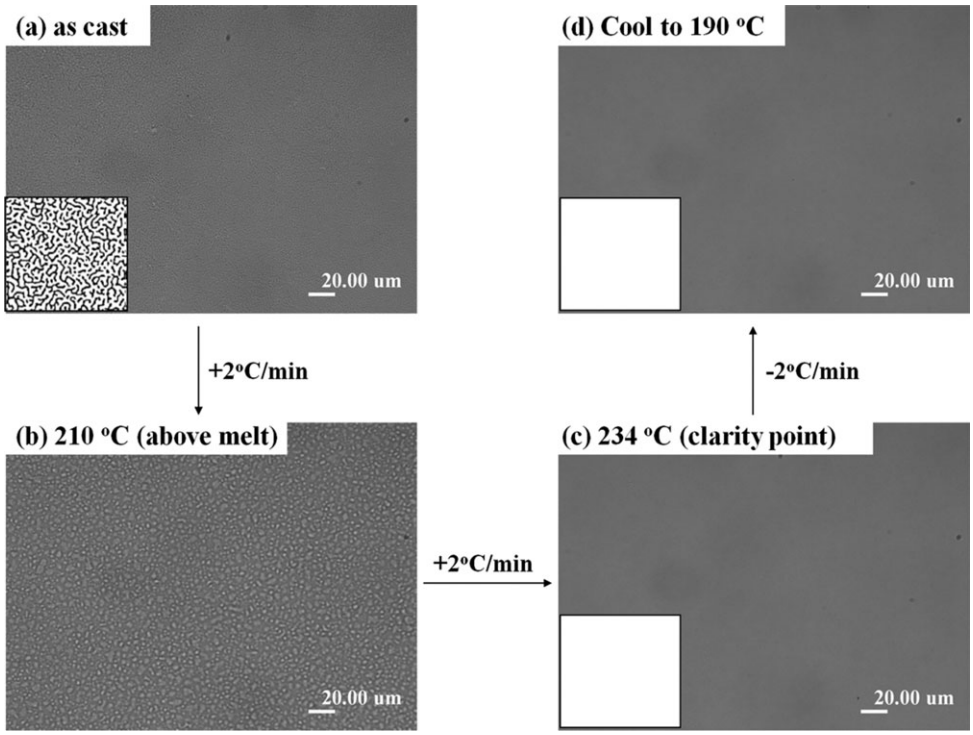

Figure 3. OM micrographs showing the phase transition during the heating and cooling cycles for the 30/70 PHB/iPMMA blend: (a) as cast, (b) heated to 210°C (above the T_m of PHB), (c) heated to 240°C (UCST), and (d) cooled to 190°C.

sPMMA blend, the phase behavior of the PHB/iPMMA blends, upon heating, also exhibited a UCST phenomenon.

Figure 4 shows the clarity points of the PHB/sPMMA and PHB/iPMMA blend systems as a function of composition to quantitatively clarify the temperature at which the blends transformed from the heterogeneous phase to the homogeneous phase. Some

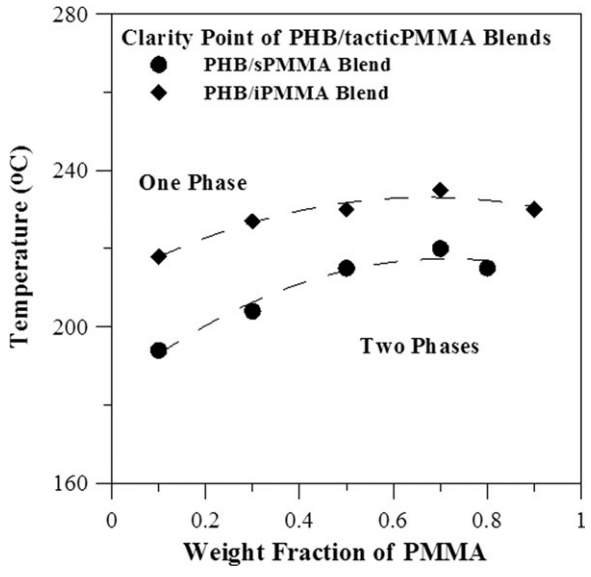

Figure 4. UCST phase diagrams for the PHB/sPMMA and PHB/iPMMA blend systems.

factors, such as the isomerism or tacticity, and the molecular weight may have influenced the phase behavior and scales of phase homogeneity in the blend. For the UCST blend system, the molecular weight of the components may have influenced its phase behavior. The blends of PHB with tactic PMMA (sPMMA and iPMMA) displayed a similar phase diagram but showed a different scale of phase homogeneity. The UCST of the PHB/iPMMA blend was higher than that of the PHB/sPMMA blend because the molecular weight of iPMMA was much higher than that of sPMMA.

Thermal characterization was performed with DSC analysis on the blend samples. Figure 5 shows the DSC traces for the PHB/sPMMA blends with different compositions quenched from below the clarity point [Figure 5(a)] and from the UCST [Figure 5(b)]. DSC analysis revealed that the quenched blends from 190°C (above the T_m of PHB but below the clarity point) showed two T_g's, which were about −4 and 100°C and were associated with the T_g values of PHB and sPMMA, respectively. The DSC result was in a good agreement with OM results and showed that at temperatures below the clarity point, the quenched blends were immiscible. However, the DSC traces in Figure 5(b) show that the blends quenched from the UCST only exhibited a single T_g, which shifted with the composition; this indicated miscibility. The cold crystallization peak temperatures of the blends quenched from the UCST [Figure 5(b)] moved toward higher temperatures with the sPMMA content, whereas the temperature of the cold crystallization peak of the blends quenched from below the clarity point [Figure 5(a)] were almost constant or shifted slightly to a higher or lower

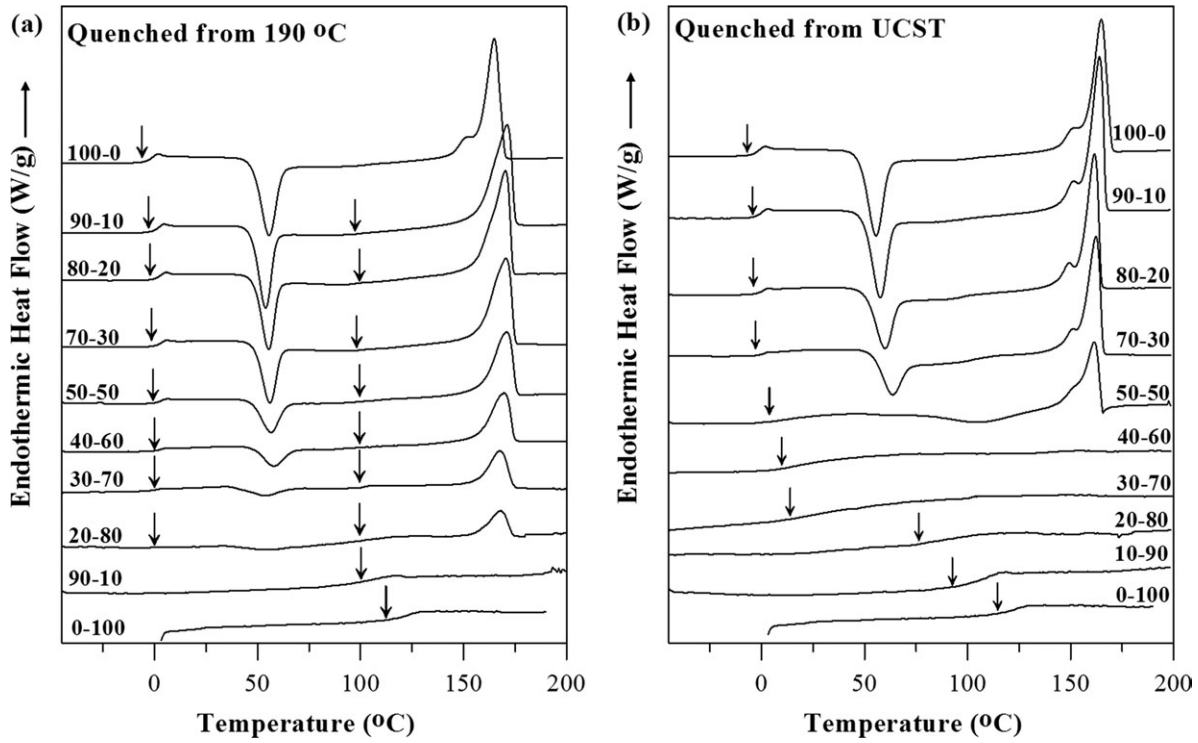

Figure 5. DSC thermographs for the PHB/sPMMA blends with different compositions during the second scan after quenching from (a) 190°C and (b) the UCST.

temperature. The shift of the cold crystallization peak temperature of the blends quenched from the UCST was considered as the crystallization process took place from a single homogeneous phase. In the homogeneous phase, as the sPMMA content increased, the viscosity of the phase also increased. Moreover, the addition of sPMMA induced a dilution effect for the PHB nuclei. The increase in the viscosity and the dilution effect caused a decrease in the overall crystallization rate and, therefore, an increase in the cold crystallization peak temperatures. In the case of the immiscible blends, the presence of noncrystallizable materials did not suffer the crystallization of PHB. Moreover, because PHB was crystallized from its own amorphous phase in the PHB-rich composition, the cold crystallization peak temperature remained almost constant at the same temperature.

For the PHB/iPMMA blend, the DSC thermographs displayed the same result as those of the PHB/sPMMA blend. Figure 6 shows the DSC traces of the PHB/iPMMA blend of different compositions quenched from below the clarity point [Figure 6(a)] and from UCST [Figure 6(b)]. DSC analysis shows that the quenched blends from 190°C (above the T_m of PHB but below the clarity point) showed a single constant T_g, which was about −4°C and was associated with the T_g of PHB at blend compositions of PHB/iPMMA of up to 30/70. This indicated that the blends were in two phases. The second T_g, which was attributed to iPMMA, could not be seen because its T_g was overlapped with the cold T_c. For blends with higher iPMMA contents, the DSC traces showed two T_g's at roughly −4 and 47°C, which corresponded to the T_g's of PHB and iPMMA, respectively. In contrast, the DSC traces in Figure 6(b) show that the blends quenched from the UCST only exhibited a single T_g dependent on the composition, and the cold crystallization peak temperatures of the quenched blends moved toward higher temperatures with increasing iPMMA content; this indicated phase homogeneity in the blends. The DSC thermographs of the PHB/sPMMA and PHB/iPMMA blends showed that blend of PHB with tactic PMMA (sPMMA and iPMMA) both exhibited the UCST phenomenon; this was in agreement with the results in the OM graphs of phase transition already shown and discussed earlier.

T_g Analysis of the UCST-Quenched Blends

The trends of T_g of the UCST-quenched samples of the PHB/sPMMA and PHB/iPMMA blends were analyzed. The values of the T_g–composition relationship for PHB/sPMMA and PHB/iPMMA are reported in Figure 7(a,b), respectively. The curves were derived by Gordon–Taylor's and Kovacs's equations. For both blend systems, when quenched from the respective UCSTs, the DSC traces exhibited a single T_g that was composition dependent. However, the values of T_g's showed a nonlinear trend. The T_g values of both blend systems could not be fitted by the Fox equation. The T_g–composition relationship of the PHB/iPMMA blend could be fitted with the Gordon–Taylor equation with a very small k value (k is an empirical fitting parameter); however, this equation could be used to fit the T_g–composition relationship of the PHB/sPMMA blend only at several compositions. The other compositions of the PHB/sPMMA blend could not be fitted with the Gordon–Taylor equation as the T_g's at compositions of 90/10 to 70/30 showed the presence of a break or a cusp. For miscible blends, there have been several theories derived to predict the T_g–composition relationship of binary blends; these include the Fox equation ($1/T_g = w_1/T_{g1} + w_2/$

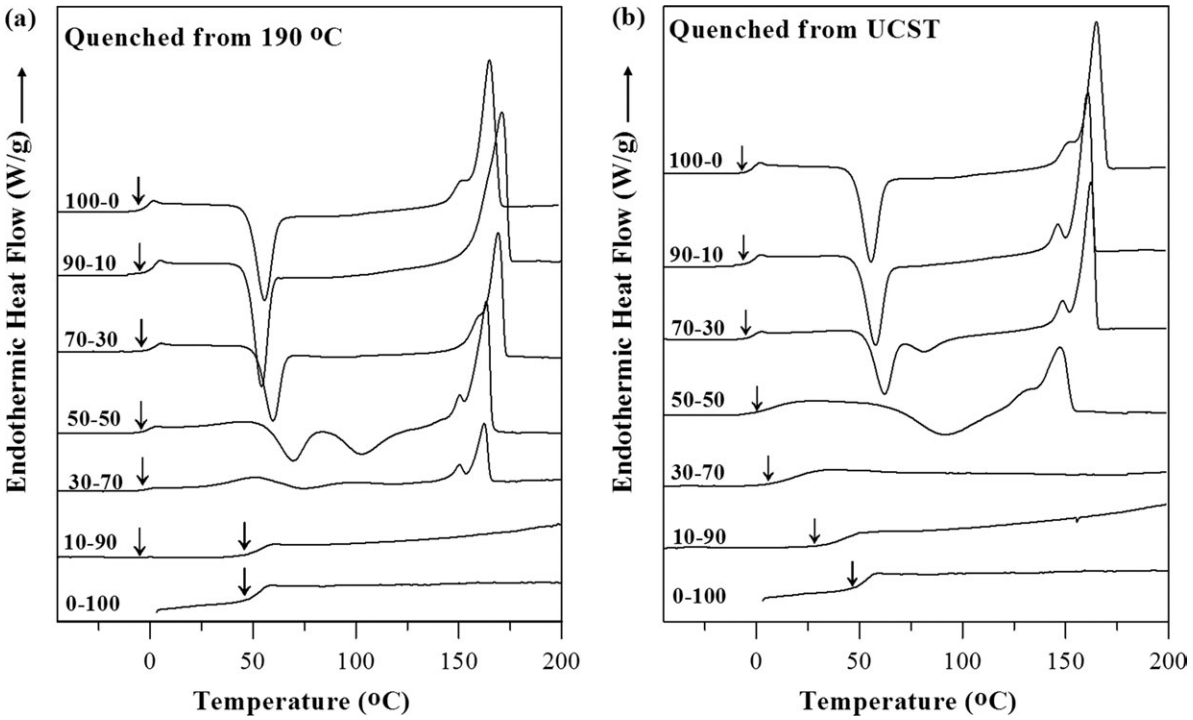

Figure 6. DSC thermographs for the PHB/iPMMA blends with different compositions during the second scan after quenching from (a) 190°C and (b) the UCST.

T_{g2}), where *wi* is the weight fraction of polymer component *i*, the Gordon–Taylor equation [$T_g = (w_1 T_{g1} + kw_2 T_{g2})/(w_1 + kw_2)$],[21] and Cauchman-Karasz[22] and Utracki.[23] These models or equations predict a monotonic T_g that is composition dependent with no cusp in the predicted curve. Other theories that could be used to predict the trends of T_g for miscible blends with the peculiar T_g–composition trends with a cusp on the T_g–composition curve have been proposed by Roy et al.,[24] Nandi et al.,[25] Aubin and Prud'homme,[26] Righetti and coworkers,[27–29] and Kovacs' theory.[30,31] Kovacs' theory explains that some blends, for which the T_g difference between two constituents is far more than 50°C, they may exhibit asymmetric T_g versus composition shapes with a discontinuity (cusp) point at intermediate compositions. This theory is based on derivation from the free-volume theory.[30] Several blends better fitted by the Kovacs T_g model have been reported. Such blend systems include polycarbonate/PCL (poly(ε-caprolactone)),[32] poly(hexamethylene sebacate)/PVPh (poly(vinyl p-phenol)),[31] and (poly (ethylene azealate)/PVPh,[31] and PEI (poly(ether imide))/PTT (poly(trimethylene terephthalate)).[33]

The following equations have been known to be used in Kovacs' theory to predict the T_g–composition relationship. The subscript 1 indicates the lower T_g component, whereas subscript 2 refers to the higher T_g component. The value of the free volume fraction of sPMMA (f_{g2}) was estimated to be 0.013,[18,34] and other relevant parameters are listed in Table I. The critical temperature was calculated to be $T_c = 81.02$°C:

$$T_c = T_{g2} - \left(\frac{f_{g2}}{\Delta\alpha_2}\right) \tag{1}$$

$$\phi_{2c} = \frac{f_{g2}}{\Delta\alpha_1\left(T_{g2} - T_{g1}\right) + f_{g2}(1 - \Delta\alpha_1/\Delta\alpha_2)} \tag{2}$$

where $\Delta\alpha_2$ is the difference between the volume expansion coefficients in the glassy and liquid states, ϕ_{2c} is the critical temperature and the corresponding critical volume fraction (relative to the polymer with higher T_g).

For

$$T_{g,x} < T_c,\ T_{g,x} = T_{g1} + \frac{\phi_2 f_{g2} + g\phi_1\phi_2}{\phi_1\Delta\alpha_1} \tag{3}$$

where $T_{g,x}$ is the glass transition temperature of the blend melt-quenched from UCST, ϕ_2 is the volume fraction of polymer 2(sPMMA), ϕ_1 is the volume fraction of polymer 1(PHB).

For

$$T_{g,x} > T_c,\ T_{g,x} = \frac{\phi_1\Delta\alpha_1 T_{g1} + \phi_2\Delta\alpha_2 T_{g2} + g\phi_1\phi_2}{\phi_1\Delta\alpha_1 + \phi_2\Delta\alpha_2} \tag{4}$$

Figure 7(a) shows that the Gordon–Taylor equation with $k = 0.45$ fit the experimental T_g–composition relationship for the PHB/sPMMA blend well only at compositions of 80 and 90 wt % sPMMA. However, all compositions of the blend could be fitted quite well with a Kovacs' equation with a value of g (g is an interaction factor) of −0.022 by showing a discontinuity point (cusp) at 80 wt % sPMMA in the blend. The negative value of the g parameter suggested that the interaction between the two constituent polymers was weaker than the interaction

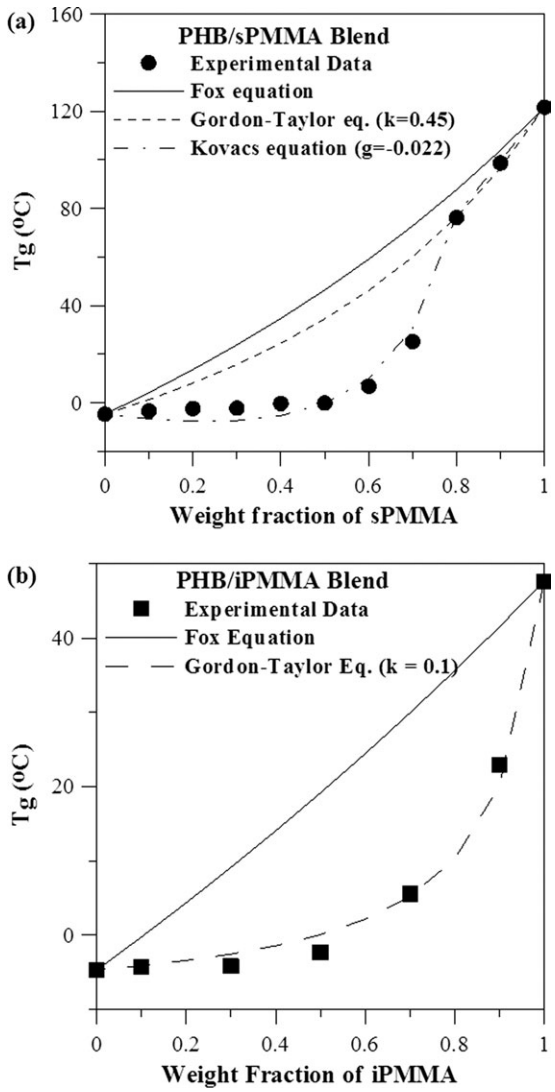

Figure 7. T_g versus composition relationships for the (a) PHB/sPMMA and (b) PHB/iPMMA blends.

between molecules of the same species. The behavior of the T_g–composition relationship of the PHB/iPMMA blend appeared to have different trends than that of the PHB/sPMMA blend. The Gordon–Taylor equation could be used to fit the trend of the T_g–composition relationship to a very small value of $k = 0.1$, as displayed in Figure 7(b). The small value of the k parameter indicated that the interaction between the two polymers was very weak in a miscible blend. From the T_g trend of the miscible blends for those two blend systems, different configurations of the polymer may have exhibited different T_g behaviors in the homogeneous phases of the blends; the two blends even both had a similar phase behavior, which was a UCST behavior.

Table I. Polymer Physical Parameters Used in the Kovacs Equation

Polymer	T_g (K)	ρ (Density) (g/cm^3)	$\Delta\alpha_i$ (K^{-1}) $\times$ 10^4
PHB	268.44	1.15[a]	4.0[b]
sPMMA	394.79	1.188[c]	3.2[c]

[a]Data from Ref. 36.
[b]Data from Ref. 37.
[c]Data from Ref. 38.

Verification of the UCST Reversibility

The UCST reversibility was also observed to confirm that the UCST was a truly physical thermodynamic process without chemical reaction, inducing the transformation from heterogeneity to homogeneity. The blend samples were first heated to a temperature above the clarity point at which the phase transition from two phases to one phase took place. When the blend samples were cooled to a temperature below the UCST and above the PHB melting point, the morphology of the blends did not revert back to phase separation; this might have been caused by the limited chain mobility of the heat-homogenized blends. Moreover, the kinetic hindrance might have impeded the long polymer chains from reorganizing into original two phases within a reasonable experimental time frame. Then, the blend samples were redissolved in chloroform, recast on a glass slide, and characterized by an OM micrograph to determine the phase reversibility. As a representative demonstration, only the results of one blend composition are shown here. Figure 8 shows the phase transition of the recast sample for the 30/70 PHB/iPMMA blend during the heating process. At ambient temperature, the recast sample graph showed several small domains; this indicated that the recast sample of the blend was in the heterogeneous phase. After it was heated to above the PHB T_m, the blend was still in the phase-separated state, as indicated by its wormlike structure. When heating was continued to a temperature above the clarity point, this induced the transformation from the heterogeneous phase to the homogeneous phase. The phase behavior during heating shown in Figure 8 was similar to the phase behavior of the original casting sample of the blends. This investigation proved that there was no chemical reaction that induced the phase transition from heterogeneity to homogeneity when the blends were heated to a temperature above the clarity point. If the chemical reaction took place in the phase transition into blend homogeneity, the blends could not revert back to the original phase separation by redissolution in chloroform.

Interaction Parameter of the Blends in the UCST Quasi-Miscible State

Another characterization was done to investigate the strength of the interaction between the two polymer blends and is also discussed. The equilibrium melting temperature of the neat PHB (T_m^0) and its blends in the UCST-quenched blends were needed to estimate interaction parameter. First, PHB and its blends were heated to above the UCST and then rapidly quenched to the desired T_c and held several times to let the PHB fully crystallize. Because the blend samples remained homogeneous when they were heated to above the UCST, as discussed previously, PHB could crystallize from the quasi-miscible state. The isothermal crystallization of neat PHB is discussed first. Figure 9(a) shows the DSC traces of the neat PHB isothermally crystallized at various T_c's through quenching from its homogeneous state. As apparently shown, the PHB component displayed two melting peaks (P_1 and P_2); upon scanning, the lend samples crystallized isothermally in a quasi-miscible state. The former melting

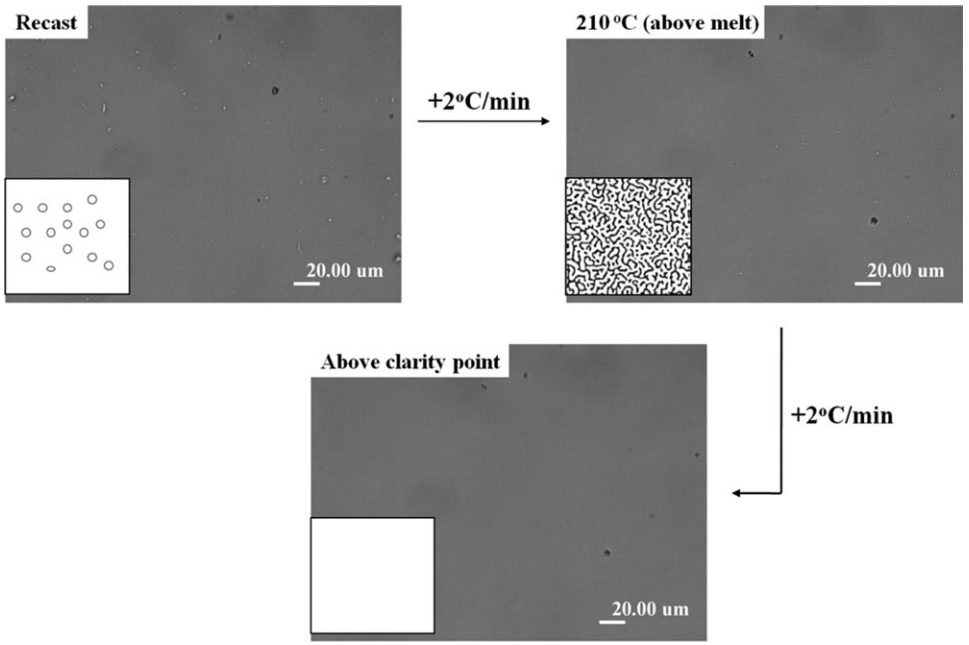

Figure 8. OM micrographs of the phase transition for the recasting of the UCST-quenched 30/70 PHB/iPMMA from phase separation to the homogeneous phase upon heating.

peak (P_1) was attributed to the melting of crystals formed isothermally at T_c, whereas the latter peak (P_2) referred to the melting of crystals through an annealing process during scanning. At a lower T_c, the crystallization process fast led to the formation of a small dimension of crystalline lamellae, which was easily suffered by the annealing process. Moreover, at a lower T_c, the scanning time from T_c to T_m was longer. Hence, the annealing process could have been more thorough. On the other hand, the lamellae formed at a higher T_c were thicker and were less easily suffered by the annealing process.[20] Both melting peaks, P_1 and P_2, increased with T_c, as shown in Figure 9(b). These two peaks were extrapolated to the $T_m = T_c$ line to obtain the values of ${T_m}^0$. For consistency, the later melting peak (P_2) of the neat PHB and blends were used for analysis with the Hoffmann–Weeks equation.

Figure 10 shows the extrapolation results of the melting peak temperature at various T_c's for several compositions of the PBH/sPMMA blend and PHB/iPMMA blend. According to the Hoffmann–Weeks procedure, the T_m values at various T_c's were extrapolated to $T_m = T_c$ to yield the values of ${T_m}^0$; these values decreased with increasing tactic PMMA content in the PHB/tactic PMMA blend. The relationship is described in the following equation:

$$T_m = \left(1 - \frac{1}{\beta}\right) T_m^0 + \frac{1}{\beta} T_c \tag{5}$$

where ${T_m}^0$ is the equilibrium melting temperature and $\beta = l/l^*$ is the ratio of the lamellar thickness l at the time of melting to the thickness l^* of the critical nucleus at T_c. The decrease in ${T_m}^0$ with a composition for the PHB blend was noted; this suggested thermodynamic miscibility between the components in the melt at ${T_m}^0$.

The interaction parameter between the PHB and tactic PMMA in the blends were obtained with the Flory–Huggins relationship described in the following equation:

$$\frac{1}{T_{mb}} - \frac{1}{T_m^0} = -\frac{RV_{2u}}{\Delta H_{2u} V_{1u}} \chi_{12} \phi_1^2 \tag{6}$$

where T_{mb} is equilibrium melting temperature for the blends, R is the universal gas constant, V_{iu} is molar volume for repeat unit i, ϕ_1 is volume fraction of tactic PMMA in the blend, ΔH_{2u} is the molar melting enthalpy for neat PHB, and χ_{12} is the polymer/polymer interaction parameter. Hence, $V_{1u} = 81.9$ cm^3/mol,[17] $V_{2u} = 75$ cm^3/mol, and $\Delta H_{2u} = 3001$ cal/mol.[35] Subscript 1 indicates the tactic PMMAs, and subscript 2 indicates PHB.

By plotting $1/T_{mb} - 1/{T_m}^0$ versus ${\phi_1}^2$, the interaction between two polymers in the blends could be estimated. The results of plotting are shown in Figure 11. The interaction parameters of both PHB/sPMMA and PHB/iPMMA showed similarly negative values of $\chi_{12} = -0.40$ and $\chi_{12} = -0.46$ for the PHB/sPMMA and PHB/iPMMA, respectively. The decrease in T_m and the negative small value of the interaction parameter confirmed that the interaction, even if it was not so strong, of the two constituents in the blend was favorable for achieving a homogeneous state above the clarity point. The value of the interaction parameters between PHB/sPMMA and PHB/iPMMA were only slightly different, with the interaction parameters for the PHB/sPMMA blend being insignificantly different from that of for the PHB/iPMMA one. It must also be pointed out here that the interaction parameters and DSC measurement values applied only to kinetically frozen states of the PHB blends (rapidly quenched from the UCST to preserve their quasi-miscible phase).

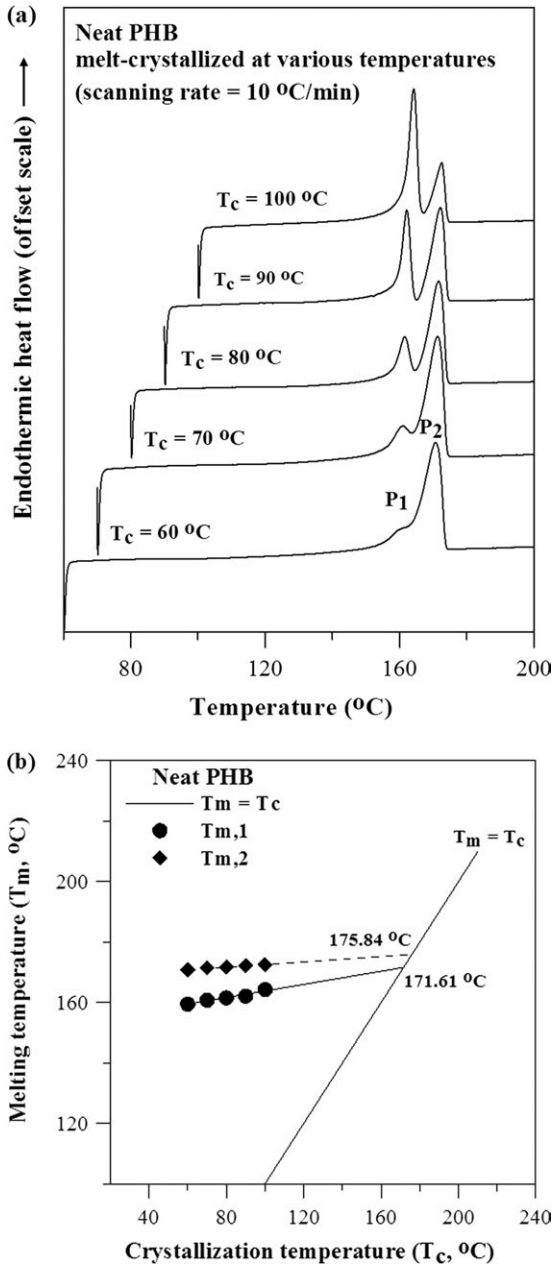

Figure 9. (a) DSC traces of the neat PHB melt-crystallized at different temperatures (T_c = 60–100°C) and (b) extrapolation with the P_1 and P_2 melting peaks to the $T_m = T_c$ line.

A comparison of the phase behavior among the different biodegradable polymers with PMMA may be informative. Another widely studied biodegradable and chiral polymer, poly(L-lactic acid), was analyzed and observed for its UCST behavior in a blend with two tactic PMMA's (sPMMA and iPMMA).[17] It was found that the PLLA/sPMMA blend showed different phase behaviors at elevated temperatures than the PLLA/iPMMA blend; the former blend showed miscibility at an elevated temperature, and the latter one displayed immiscibility. However, the phase behavior of the PLLA/sPMMA blend was similar to that of the PLLA/aPMMA blend; this is probably not surprising as aPMMA is mostly composed of higher percentages of sPMMA mers than iPMMA mers. Apparently, the oppositely configured sPMMA tended to have more intimate interactions with the chiral PLLA than did iPMMA with PLLA. This was caused by the difference in the chain configuration of sPMMA and iPMMA. That is, the effect of the PMMA tacticity was quite pronounced in interactions and miscibility between PMMA and PLLA.

By comparison, there also existed a PMMA tacticity effect on the phase behavior of PHB/PMMA; however, the effect tended to be relatively less pronounced in the PHB/PMMA blends. sPMMA and iPMMA showed a big difference in the chain configuration, but the blends of tactic PMMA with PHB showed similar phase behavior when the blends were heated at elevated temperatures above the UCST. All those PHB/sPMMA or PHB/iPMMA blends were immiscible systems, only exhibiting a UCST upon heating to certain higher temperatures; these differed in their phase diagrams to certain extents because of differences in either the tacticity or molecular weights. This may have been because the chiral configuration in PHB was physically less prominent and more diffused than that of PLLA; this led to a less pronounced interaction effect between the PHB/sPMMA and PHB/iPMMA pairs.

Crystalline Morphology of the Blends

As discussed previously, the tactic PMMA effect on the phase behavior and interactions in the amorphous domains of the PHB/PMMA blend was not significant. It might be worthwhile to examine the possible effect of the PMMA tacticity on the PHB/tactic PMMA spherulitic morphology. We observed the spherulitic morphology of the blends by holding the PHB/tactic PMMA blend samples at temperatures above their respective clarity points; then, they were quickly cooled to an isothermal T_c for full crystallization to develop a final spherulitic pattern. Several blend compositions were investigated; for brevity, only several PHB-rich compositions are shown here as representative samples. Figure 12 shows a summary of the polarized optical micrographs for spherulitic birefringence signs (positive or negative types) and ring-banded/ringless patterns of the PHB/iPMMA blend (top) or PHB/sPMMA blend (bottom) with respect to the variations in T_c and blend composition. For the PHB/iPMMA blend (top portion of Figure 12), only positively birefringent spherulites were present at all T_c's and compositions. Ring-banded spherulites occurred in a range of T_c's and blend compositions, whereas ringless spherulites occurred in another range, as shown in the graphs, but all ringless or ring-banded spherulites had the same positively birefringence sign. By comparison, the bottom portion of Figure 12 shows that the variation trend of the spherulitic morphology of the PHB/sPMMA blend differed significantly from that of the PHB/iPMMA blend. For the PHB/sPMMA blend, negatively and positively birefringent spherulites were present at different ranges of T_c or compositions. The ring-banded spherulites occurred in a range of T_c's and blend compositions (i.e., higher T_c and lower sPMMA contents), whereas ringless spherulites occurred in another range (i.e., lower T_c's and higher sPMMA contents), as shown in the graphs. However, all of the ringless spherulites had a negative birefringence sign,

Applied Polymer SCIENCE

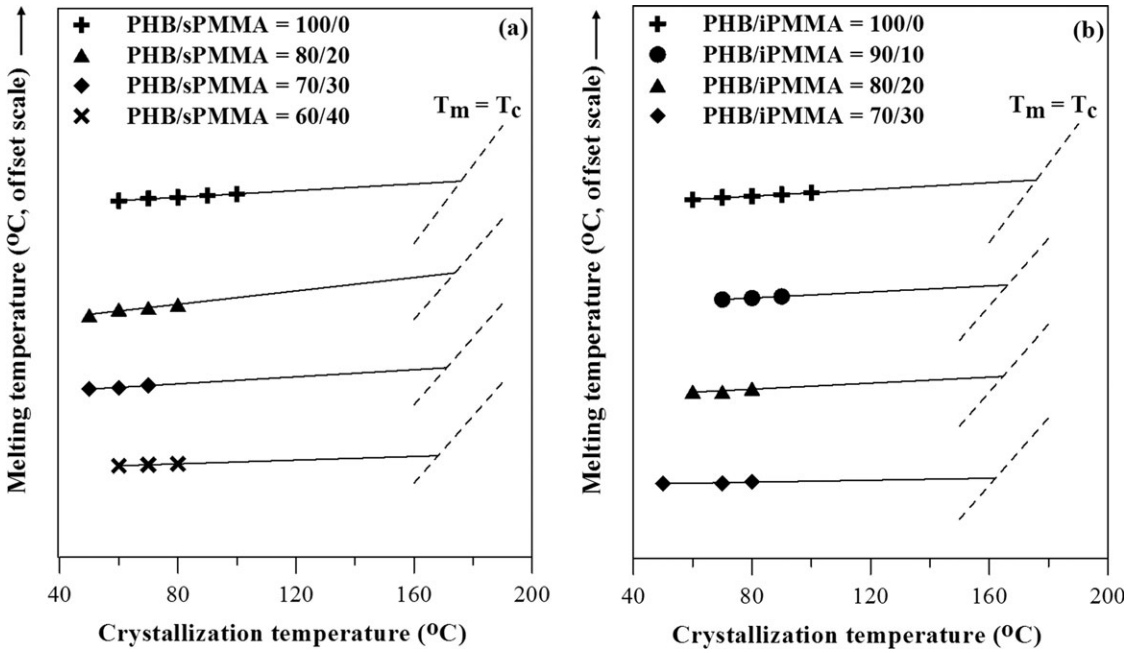

Figure 10. Hoffmann–Weeks plots of the (a) PHB/sPMMA and (b) PHB/iPMMA blends for several compositions melt-crystallized at various T_c's.

whereas all of the ring-banded spherulites had the opposite positive birefringence sign. Apparently, the PHB/sPMMA blend exhibited a crystalline morphology (with respect to T_c and composition), which differed significantly from the PHB/iPMMA blend.

Additional information for the birefringence of spherulites is given here. According to the optical birefringence character, polymer spherulites can be classified as negative- or positive-type spherulites. A spherulite that shows blue color in its first and third quadrants is called a negatively birefringent spherulite.

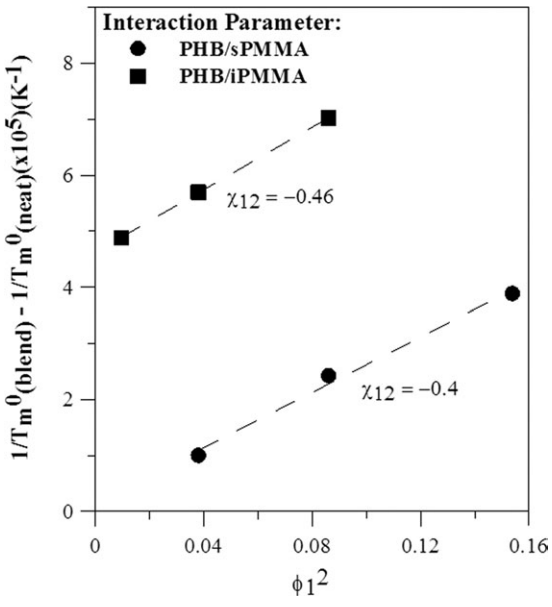

Figure 11. Interaction parameter of the UCST-quenched PHB/sPMMA and PHB/iPMMA blends (different symbols) by T_m depression.

A positively birefringent spherulite shows orange color in its first and third quadrants. A negatively birefringent spherulite gives a higher refractive index in the tangential direction (n_t) compared to the refractive index in the radial direction (n_r). On the other hand, a positively birefringent spherulite has a value of $n_r > n_t$, where n refers to the refractive index of crystals and the subscripts r and t refer to the radial and transverse directions of polymer chains in the spherulite.

To follow up the analysis of crystalline morphology and the possible effect of the PMMA tacticity on the crystalline morphology of the PHB/tactic PMMA blends, crystalline spherulites phase diagrams as functions of the tacticity, composition, and crystallization were constructed. Figure 13 shows the crystallization and composition ranges for the spherulite birefringence signs (positive/negative) and ring-banded/ringless patterns for the PHB/iPMMA and PHB/iPMMA blends. The bottom line (PMMA content = 0) on each of the two phase diagrams [Figure 13(a,b)] indicates the spherulite patterns of the neat PHB, which exhibit ringless and positively birefringent spherulites at $T_c = 50°C$ or lower. However, ring-banded and positively birefringent spherulites were observed at $T_c = 60°C$ or higher up to 90°C. That is, regardless of the ringless or ring-banded patterns, the spherulites in neat PHB had only positively birefringence signs. Figure 13(a) shows that the PHB/iPMMA blends at all three compositions (10, 20, and 30 wt % iPMMA), when crystallized at any T_c, pretty much showed the same positive birefringence as neat PHB, except that the ring-banded spherulites for the PHB/iPMMA blend occurred at slightly different T_c ranges (depending on compositions) from that for neat PHB. However, by dramatic contrast, the sPMMA exerted a significant effect on the PHB spherulite morphology when sPMMA was blended into PHB. The phase diagram of Figure 13(b) showed clearly that at high

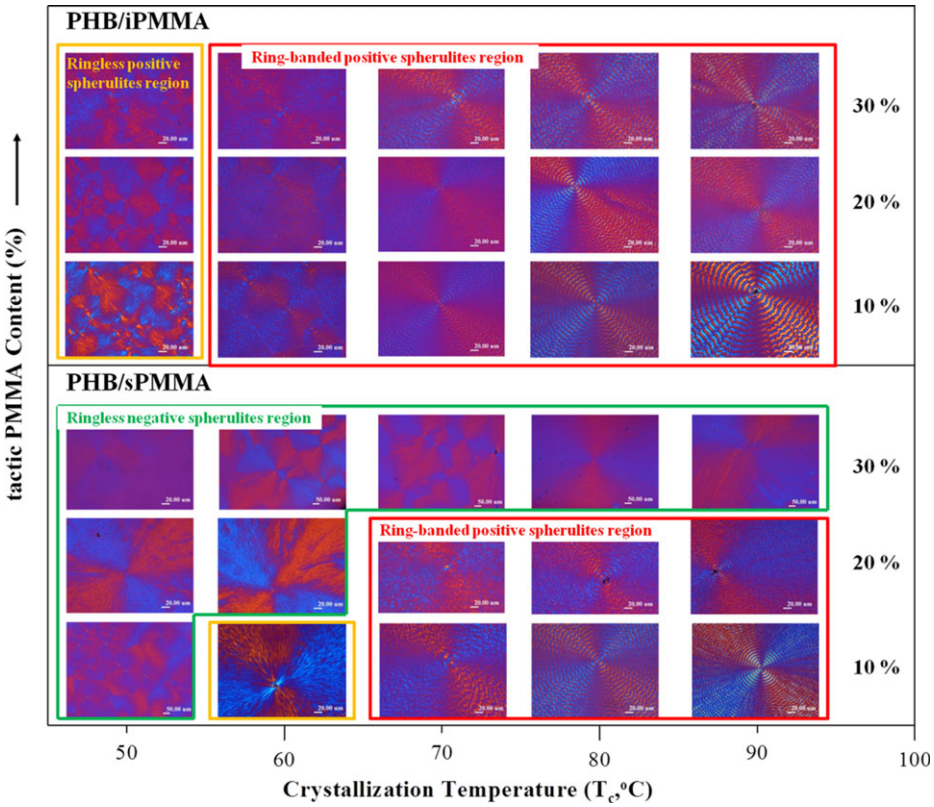

Figure 12. Spherulite birefringence (positive or negative) and ring-banded/ringless patterns of the PHB/iPMMA blend (top) and PHB/sPMMA blend (bottom) with respect to the variation of T_c and the blend compositions. [Color figure can be viewed in the online issue, which is available at wileyonlinelibrary.com.]

sPMMA contents (e.g., 30 wt %) in the PHB/sPMMA blend, the spherulites were all negatively birefringent and ringless when crystallized at any T_c between 50 and 90°C. That is, not only was the original ring-banded pattern in the neat PHB spherulites completely disrupted, but the optical sign also reverted completely from positive to negative when 30 wt % sPMMA was blended into PHB. Even at lower contents (10 and 20 wt %) of sPMMA in the PHB/sPMMA blend, the altering effect on the original positive birefringence and disruption of the ring-banded pattern of the spherulites was easily observable. This syndiotacticity effect on altering the PHB crystalline morphology was not seen in iPMMA. For example, in the PHB/iPMMA blend [Figure 13(a)], the optical sign remained positively birefringent, and the spherulite pattern remained ring-banded when iPMMA at 10, 20, and 30 wt % were blended into PHB; this was the same as that in neat PHB.

CONCLUSIONS

This study on blends of chiral PHB with tactic sPMMA or iPMMA showed results of tacticity influence on the PHB/PMMA blends' phase and crystalline morphology, to a lesser extent on the amorphous phase behavior but with a stronger influence on the crystalline morphology. The blends were both immiscible at ambient temperature and transformed to the miscible state when they were heated to elevated temperatures above the clarity point, and they did not revert back to phase separation when they were cooled to a temperature below the PHB T_m; this might have been caused by the limited chain mobility of the UCST-homogenized blend. There was no chemical reaction leading to the phase transition from the heterogeneous to homogeneous state, as clarified in the UCST reversibility discussion. The phase diagram of the two blends displayed a difference in the cloud temperatures because of the different molecular weights of the amorphous polymer. Specifically, the interaction parameters and DSC measured values applied only to the kinetically frozen states of the PHB blends (rapidly quenched from UCST to preserve their quasi-miscible phase). The PMMA tacticity effect on the amorphous phase of the PHB/PMMA blends in this study was less prominent than that seen in PLLA/tactic PMMA blends previously reported in the literature. This may have been because the chiral configuration in PHB was physically less prominent and more diffused than PLLA, and this led to a less pronounced interaction effect between the PHB/sPMMA and PHB/iPMMA pairs.

In dramatic contrast, the PMMA tacticity effect was quite prominent in the crystalline phase of the PHB/tactic PMMA blends. The sPMMA exerted a significant effect on the PHB spherulite morphology when sPMMA was blended

Applied Polymer SCIENCE

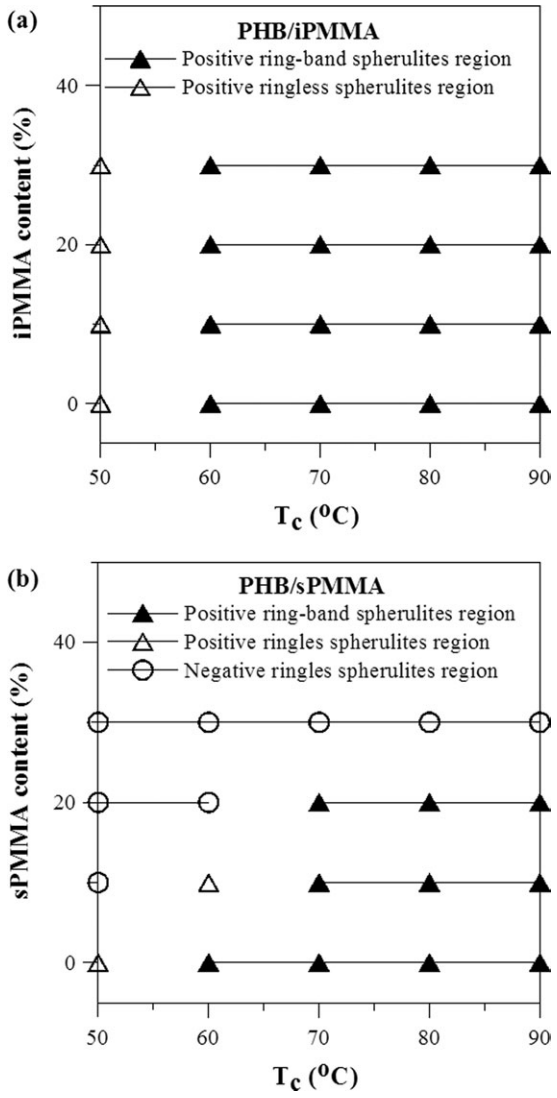

Figure 13. Crystallization and composition ranges for the spherulite birefringence signs (positive or negative) and ring-banded/ringless patterns for the (a) PHB/iPMMA blend (top) and (b) PHB/sPMMA blend (bottom): (▲) ring-banded with positive birefringence, (△) ringless with positive birefringence, and (○) ringless with negative birefringence.

into PHB. At high sPMMA contents (e.g., 30 wt %) in the PHB/sPMMA blend, the spherulites were all negatively birefringent and ringless when they were crystallized at any T_c between 50 and 90°C. That is, not only was the original ring-banded pattern in the neat PHB spherulites completely disrupted, but the optical sign also reverted completely from positively to negatively birefringent when 30 wt % sPMMA was blended into PHB. This syndiotacticity effect on altering the PHB crystalline morphology was not seen in iPMMA.

ACKNOWLEDGMENTS

This work was financially supported by a basic research grant (NSC-97-2221-E-006-034-MY3) for three consecutive years from Taiwan's National Science Council, to which the authors express their gratitude.

REFERENCES

1. Avella, M.; Martuscelli, E. *Polymer* **1988**, *29*, 1731.
2. Avella, M.; Martuscelli, E.; Raimo, M. *Polymer* **1993**, *34*, 3234.
3. Yoon, J. S.; Choi, C. S.; Maing, S. J.; Choi, H. J.; Lee, H. S.; Choi, S. *J. Eur. Polym. J.* **1993**, *29*, 1359.
4. You, J. W.; Chiu, H. J.; Don, T. M. *Polymer* **2003**, *44*, 4355.
5. Blümm, E.; Owen, A. *J. Polymer* **1995**, *36*, 4077.
6. Nurkhamidah, S.; Woo, E. M. *Ind. Eng. Chem. Res.* **2011**, *50*, 4494.
7. Hsieh, Y. T.; Woo, E. M. *Express Polym. Lett.* **2011**, *5*, 570.
8. Shetter, J. A. *J. Polym. Sci. Part B: Polym. Lett.* **1963**, *1*, 209.
9. O'Reilly, J. M.; Bair, H. E.; Karasz, F. E. *Macromolecules.* **1982**, *15*, 1083.
10. Plazek, D. J.; Raghupathi, N. *Polym. Prepr. Am. Chem. Soc. Div. Polym. Chem.* **1974**, *15*, 53.
11. Roerdink, E.; Challa, G. *Polymer* **1978**, *19*, 173.
12. Schurer, J. W.; De Boer, A.; Challa, G. *Polymer* **1975**, *16*, 201.
13. Vorenkamp, E. J.; Brinke, G. T.; Meijer, J. G.; Jager, H.; Challa,G. *Polymer* **1985**, *26*, 1725.
14. Hsu, W. P. *J. Appl. Polym. Sci.* **1997**, *66*, 1773.
15. Hsu, W. P. *J. Appl. Polym. Sci.* **2002**, *83*, 1425.
16. Li, S. H.; Woo, E. M. *Polym. Int.* **2008**, *57*, 1242.
17. Li, S. H.; Woo, E. M. *J. Polym. Sci. Part B: Polym. Phys.* **2008**, *46*, 2355.
18. Siciliano, A.; Seves, A.; Marco, D. T.; Cimmino, S.; Martuscelli, E.; Silvestre, C. *Macromolecules* **1995**, *28*, 8065.
19. Cimmino, S.; Iodice, P.; Silvestre, C.; Karasz, F. E. *J. Appl. Polym. Sci.* **2000**, *75*, 746.
20. Cimmino, S.; Iodice, P.; Martuscelli, E.; Silvestre, C. *Thermochim. Acta.* **1998**, *321*, 89.
21. Gordon, M.; Taylor, J. S. *J. Appl. Chem.* **1952**, *2*, 493.
22. Couchman, P. R.; Karasz, F. E. *Macromolecules* **1978**, *11*, 117.
23. Utracki, L. A. *Adv. Polym. Technol.* **1985**, *5*, 33.
24. Roy, S. K.; Brown, G. R.; St-Pierre, L. E. *Int. J. Polym. Mater.* **1983**, *10*, 13.
25. Nandi, A. K.; Mandal, B. M.; Bhattacharyya, S. N.; Roy, S. K. *Polym. Commun.* **1986**, *27*, 151.
26. Aubin, M.; Prud'homme, R. E. *Macromolecules* **1988**, *21*, 2945.
27. Righetti, M. C.; Ajroldi, G.; Pezzin, G. *Polymer* **1992**, *33*, 4779.
28. Righetti, M. C.; Ajroldi, G.; Pezzin, G. *Polymer* **1992**, *33*, 4786.
29. Righetti, M. C.; Ajroldi, G.; Marchionni, G.; Pezzin, G. *Polymer* **1993**, *34*, 4307.
30. Kovacs, A. *J. Adv. Polym. Sci.* **1963**, *3*, 394.
31. Woo, E. M.; Chiang, C. P. *Polymer* **2004**, *45*, 8415.
32. Cheung, Y. W.; Stein, R. S. *Macromolecules.* **1994**, *27*, 2512.

33. Kuo, Y. H.; Woo, E. M.; Kuo, T. Y. *Polym. J.* **2001**, *33*, 920.
34. O'Connor, K. M.; Scholsky, K. M. *Polymer* **1989**, *30*, 461.
35. Hasan, A. A. *Polym. Bull.* **1998**, *41*, 593.
36. Bharam, P. J.; Keller, A.; Otun, E. L.; Holmes, P. A. *J. Mater. Sci.* **1984**, *19*, 2781.
37. Van Krevelen, D. W. Properties of Polymers: Correlations with Chemical Structure; Elsevier: Amsterdam, **1976**.
38. Wunderlich, W. In Polymer Handbook; Brandrup, J., Immergut, E. H., Grulke, E. A., Eds.; Wiley: New York, **1999**; Vol. *5*, p 87.